Draft version November 15, 2012
Preprint typeset using LaTeX style emulateapj v. 5/2/11

A SUCCESSFUL BROAD-BAND SURVEY FOR GIANT Lyα NEBULAE II: SPECTROSCOPIC CONFIRMATION

Moire K. M. Prescott[1,2], Arjun Dey[3], Buell T. Jannuzi[3]

Draft version November 15, 2012

ABSTRACT

Using a systematic broad-band search technique, we have carried out a survey for large Lyα nebulae (or Lyα "blobs") at $2 \lesssim z \lesssim 3$ within 8.5 square degrees of the NOAO Deep Wide-Field Survey (NDWFS) Boötes field, corresponding to a total survey comoving volume of $\approx 10^8$ h_{70}^{-3} Mpc^3. Here, we present our spectroscopic observations of candidate giant Lyα nebulae. Of 26 candidates targeted, 5 were confirmed to have Lyα emission at $1.7 \lesssim z \lesssim 2.7$, four of which were new discoveries. The confirmed Lyα nebulae span a range of Lyα equivalent widths, colors, sizes, and line ratios, and most show spatially-extended continuum emission. The remaining candidates did not reveal any strong emission lines, but instead exhibit featureless, diffuse blue continuum spectra. Their nature remains mysterious, but we speculate that some of these might be Lyα nebulae lying within the redshift desert (i.e., $1.2 \lesssim z \lesssim 1.6$). Our spectroscopic follow-up confirms the power of using deep broad-band imaging to search for the bright end of the Lyα nebula population across enormous comoving volumes.

Subject headings: galaxies: formation — galaxies: evolution — galaxies: high-redshift — surveys

1. INTRODUCTION

Giant radio-quiet Lyα nebulae (also know as "Lyα blobs") provide a window into the physics of ongoing massive galaxy formation (e.g., Francis et al. 1996; Ivison et al. 1998; Steidel et al. 2000; Palunas et al. 2004; Matsuda et al. 2004; Dey et al. 2005; Saito et al. 2006; Nilsson et al. 2006; Smith & Jarvis 2007; Prescott et al. 2009; Yang et al. 2009). Rare systems found primarily in overdense regions (Prescott et al. 2008; Matsuda et al. 2004, 2005, 2011; Saito et al. 2006; Yang et al. 2009, 2010), Lyα nebulae are extremely luminous ($L_{Ly\alpha} \sim 10^{44}$ erg s^{-1}) and are frequently associated with young, star-forming galaxy populations or obscured AGN (e.g., Basu-Zych & Scharf 2004; Matsuda et al. 2004; Dey et al. 2005; Geach et al. 2007, 2009; Prescott et al. 2012b). Theoretical and observational investigations into the power source behind Lyα nebulae have painted a varied picture, presenting arguments for AGN powering (Chapman et al. 2004; Basu-Zych & Scharf 2004; Geach et al. 2007, 2009), starburst-driven winds (Taniguchi & Shioya 2000; Taniguchi et al. 2001; Matsuda et al. 2004), spatially-extended star formation (Matsuda et al. 2007; Prescott et al. 2012b), cold accretion (Nilsson et al. 2006; Smith et al. 2008; Goerdt et al. 2010; Faucher-Giguère et al. 2010; Rosdahl & Blaizot 2012), or some combination thereof (Dey et al. 2005; Prescott et al. 2009, 2012b; Webb et al. 2009; Colbert et al. 2011). Larger samples of giant radio-quiet Lyα nebulae drawn from unbiased surveys are needed in order to accurately measure the space density of these sources, to determine the emission mechanisms primarily responsible for the Lyα nebula class as a whole, and to understand their relationship to the more well-studied Lyα haloes found around many high redshift radio galaxies (e.g., McCarthy 1993, and references therein; van Ojik et al. 1996; Weidinger et al. 2005; Miley et al. 2006; Barrio et al. 2008; Smith et al. 2009; Zirm et al. 2009).

Increasing the sample of such a rare class of objects requires surveying large comoving volumes, but the standard approach relying on narrow-band imaging is limited by observational expense. Our complementary approach was to design a new search technique using deep *broad-band* imaging (Prescott 2009). We employed this method to select a sample of Lyα nebula candidates from the Boötes Field of the NOAO Deep Wide-Field Survey (NDWFS; Jannuzi & Dey 1999). A full presentation of our survey algorithm as well as the selection function of this approach and the implications for the space density of Lyα nebulae can be found in companion papers (Prescott et al. 2012a, 2013, in preparation; hereafter, Papers I and III, respectively).

In this work (Paper II), we focus on the spectroscopic follow-up of Lyα nebula candidates drawn from deep archival broad-band imaging of the NDWFS Boötes field. In Section 2, we give a brief outline of the survey design and candidate sample. In Section 3, we discuss our spectroscopic observations and reductions. Section 4 presents the 5 Lyα nebulae discovered within this 8.5 square degree survey and discusses our primary contaminant sources, potentially an interesting population in their own right. Section 5 discusses the implications of this sample, and we conclude in Section 6.

We assume the standard ΛCDM cosmology ($\Omega_M = 0.3$, $\Omega_\Lambda = 0.7$, $h = 0.7$); $1''$ corresponds to a physical scales of 8.3-7.8 kpc for redshifts of $z = 1.2 - 2.9$. All magnitudes are in the AB system (Oke 1974).

2. SEARCH DESIGN

We have designed an innovative search for Lyα nebulae in deep broad-band imaging and applied it to the

[1] TABASGO Postdoctoral Fellow; Department of Physics, Broida Hall, Mail Code 9530, University of California, Santa Barbara, CA 93106; mkpresco@physics.ucsb.edu
[2] Steward Observatory, University of Arizona, 933 N. Cherry Avenue, Tucson, AZ 85721
[3] National Optical Astronomy Observatory, 950 North Cherry Avenue, Tucson, AZ 85719

NDWFS Boötes field (Paper I). Our search is most sensitive to the largest and brightest Lyα nebulae because it leverages the deep blue (B_W) imaging of NDWFS to look for sources where bright Lyα emission boosts the broad-band flux relative to the very dark sky. Thanks to the wide area ($\approx$9 deg^2) of the NDWFS and the large width of the B_W filter ($\approx$ 1275Å, corresponding to $\Delta z \approx 1$), our survey is able to probe an enormous comoving volume ($\approx 10^8$ h$_{70}^{-3}$ Mpc^3) with archival data and significantly reduce the required observational overhead. Our survey is therefore complementary to smaller volume surveys for Lyα nebulae that rely on sensitive narrow-band imaging (e.g., Matsuda et al. 2004; Saito et al. 2006; Smith & Jarvis 2007; Yang et al. 2009, 2010; Matsuda et al. 2011).

The search algorithm and candidate sample are discussed in detail in Paper I. In brief, we selected giant Lyα nebula candidates using wavelet analysis of the compact-source-subtracted B_W images. We selected a set of first and second priority candidates (Figure 1) based on their $B_W - R$ color, as measured using large 30 pix=7.7″ diameter apertures, and wavelet size, as determined using SourceExtractor (Bertin & Arnouts 1996) on the wavelet-deconvolved images. The final candidate sample consisted of 39 first priority and 40 second priority sources over a search area of 8.5 square degrees. Both first and second priority samples contained candidates with diffuse morphologies (morphological category DIFFUSE) as well as those that appear to be tight groupings of compact sources (morphological category GROUP), as discussed in Paper I. In addition, we flagged 6 sources from outside these selection regions that showed promising morphologies (third priority).

3. SPECTROSCOPIC FOLLOW-UP

In this section we describe the spectroscopic follow-up of the Lyα nebula candidate sample.

3.1. *Observations & Reductions*

We targeted a total of 26 Lya nebula candidates (15 first priority, 5 second priority, and all 6 third priority candidates). Longslit spectroscopic observations were obtained using the MMT and the Blue Channel Spectrograph during 2007 May, 2008 April and June (Table 1). The observations used the 300 l/mm grating with 1.″0/1.″5 wide slits resulting in a resolution FWHM of 2.6/3.4Å and a wavelength range of $\Delta\lambda \approx 3100 - 8320$Å.

During our 2007 run, we chose slit orientations based primarily on the morphology of the candidate (i.e., aligned with the major axis of the emission as estimated from the B_W-band morphology), and as a secondary criterion attempted to intersect a nearby bright reference object if possible. In practice, however, we found that the faintness of our candidates and the short duration of our spectroscopic exposures necessitated a positional reference. As a result, slit orientations during the 2008 runs were chosen to always include a positional reference object, and consequently do not always trace the major axis of the B_W morphology. During these later runs, we dithered the target along the slit by $\approx 5''$ between exposures to minimize the effect of any bad pixels. The full list of targeted candidates and the results of the spectroscopic observations are given in Table 2.

We reduced the spectroscopic data using IRAF.[4] We subtracted the overscan and bias, and applied a flat-field correction using normalized observations of the internal quartz flat-field lamps. Twilight flats were used to determine the illumination correction for the science frames. We removed cosmic rays from the 2D sky-subtracted data using *xzap*.[5] One-dimensional spectra were generated using the task *apall* and optimal variance-weighted extraction (Valdes 1992); the spectral trace was determined using bright unresolved sources on the slit. We determined the wavelength solution to an rms precision of $\approx$0.08-0.18Å using HeArNe and HgCd comparison lamps, and then corrected the data for any slight systematic offset using the night sky lines as a reference. The final wavelength calibration is accurate to $\pm$0.42Å. The relative flux calibration was based on observations of the standard stars BD+33 2642, BD+26 2606, BD+28 4211, Feige 34, and Wolf 1346.[6] For each night, we applied a grey shift to compensate for any variable grey (i.e., independent of wavelength) extinction that may have affected a given standard star observation relative to one taken under better conditions. The sensitivity functions derived from individual standard star exposures were consistent to within $\lesssim$0.1 mag.

Due to the faintness of the candidates and the fact that we are searching for luminous Lyα nebulae at $z \approx 2-3$, the aim of our follow-up spectroscopic program was to look for strong, high equivalent width line emission. A single strong line in the blue can be identified as Lyα rather than an unresolved [O II]$\lambda\lambda$3726,3729 doublet (the only other possibility at these wavelengths) due to the fact that a detection of [O II] would be accompanied by stronger detections of [O III]$\lambda\lambda$4959,5007 and Hα as well. Candidates with strong Lyα emission at $z \approx 2-3$ in the B_W-band are easily detectable with the MMT/Blue Channel down to a 5σ limit of $\approx 1-7\times10^{-17}$ in 30 minutes (assuming a FWHM$_{obs}$ = 12Å Lyα line measured within a 1.″5×5″ aperture). This corresponds to limiting line luminosities of $\approx 0.3-5\times10^{42}$ erg s^{-1}, which are below the typical luminosities of giant Lyα nebulae. However, continuum-only sources are much fainter and require longer integration times to yield high signal-to-noise ratio spectra, more than was available during our spectroscopic campaign. To allow us to target the largest number of candidates, we therefore carried out a quick reduction of the data in real-time and continued integrating on each of the 26 targeted candidates up until the point where we could either confirm the presence of a line or confirm the presence of continuum with no strong lines. The deeper spectroscopy necessary for studying the spectral properties of our confirmed Lyα nebulae in detail as well as for detecting absorption features in continuum-only sources is left to future observations with larger telescopes.

4. RESULTS

Of the 15 first priority and 5 second priority candidates targeted for spectroscopic follow-up, 4 first priority

[4] IRAF is distributed by the National Optical Astronomy Observatories, which are operated by the Association of Universities for Research in Astronomy, Inc., under cooperative agreement with the National Science Foundation.

[5] http://iraf.noao.edu/iraf/ftp/iraf/extern/xdimsum020627

[6] KPNO IRS Standard Star Manual

sources and 1 second priority source had confirmed Lyα emission: we easily recovered the previously-discovered large Lyα nebula at $z \approx 2.66$ (LABd05; Dey et al. 2005) and discovered new, spatially-extended Lyα nebulae at $z \approx 1.67$, $z \approx 1.88$, $z \approx 2.14$, and $z \approx 2.27$. In addition, we also targeted 6 third priority candidates that showed promising diffuse morphologies upon visual inspection. However, no Lyα or [O II] line emission was confirmed in any of the third priority candidates. In this section, we describe each of the confirmed sources in turn and then discuss the primary contaminants to our survey.

4.1. *Confirmed Lyα Sources*

Figures 2-6 show the postage stamps, two-dimensional spectra, and one-dimensional spectra of the Lyα sources; the measured properties are listed in Table 3. The spectral extraction apertures were chosen to maximize the signal-to-noise ratio of Lyα. Redshifts were determined from the centroid of a Gaussian fit to the observed Lyα line. No correction was included for Lyα absorption, a potential source of bias in our redshift estimates. The B_W sizes, isophotal areas, and surface brightnesses were measured above the median 1σ surface brightness limit of the entire NDWFS survey from the original B_W images using SourceExtractor (DETECT_MINAREA=5, DETECT_THRESH=28.9 mag arcsec^{-2}; Bertin & Arnouts 1996). The Lyα sizes were measured from the 2D spectra using SourceExtractor above the 1σ surface brightness limit at the location of Lyα (DETECT_MINAREA=5, DETECT_THRESH$\approx 1\times10^{-18}$ erg s^{-1} cm^{-2} Å^{-1} arcsec^{-2}; see Table 3). The B_W sizes along the slit can underestimate the Lyα sizes measured from the 2D spectra; in the case of PRG3, our deepest spectrum, the B_W size underestimates the Lyα size by a factor of $\gtrsim$1.3.

Estimates for the total Lyα isophotal area and total Lyα luminosity are also given in Table 3. The approximate total Lyα isophotal area was estimated by correcting A_{B_W} by a factor of ν^2, where A_{B_W} is the isophotal area of the source on the B_W image and ν is the ratio of the Lyα and B_W sizes measured along the slit. The approximate total Lyα luminosity was derived by scaling the Lyα luminosity within the spectroscopic aperture by the geometric correction factor $f_{geo} = A_{B_W} \times \nu^2/(\omega \times d)$, where ω is the slit width and d is the spatial extent of the spectral extraction aperture. We stress, however, that in using area corrections based on broad-band imaging we are relying on the assumptions that the B_W emission roughly traces the Lyα emission in the source and that the relative factor between the B_W and Lyα sizes is the same throughout the object as it is along the slit; either of these assumptions may be violated in practice.

In what follows, we discuss each confirmed Lyα source in detail. Of the confirmed Lyα nebulae, four were originally categorized as having a DIFFUSE morphology while one (PRG4) was categorized as having a GROUP morphology (see Paper I).

4.1.1. *PRG1*

PRG1 is a remarkable Lyα nebula (Figure 2). As discussed in Prescott et al. (2009), it is the first example of a Lyα nebula with strong, spatially-extended He II emission and weak metal lines, suggestive of a hard ionizing continuum and potentially low metallicity gas. The B_W imaging shows a diffuse nebula and several compact sources, the brightest of which is located at the northwest edge of the nebula. Despite the strong Lyα emission and large size (>78 kpc), PRG1 was selected as a second priority candidate because, at $z \approx 1.67$, Lyα is at the edge of the optical window and not contained within the B_W band, giving the source a relatively red $B_W - R$ color. Thanks to its diffuse blue continuum (95%) and He II emission (5%), however, this source was still selected by our survey. When first discovered, this source was the lowest redshift Lyα nebula known and the only one that shows strong spatially-extended He II emission; PRG1 is therefore an ideal target for detailed study of the physical conditions and kinematics within Lyα nebulae. Analysis of the metallicity and source of ionization in PRG1 is given in Prescott et al. (2009), and more detailed analysis using deep Keck/LRIS spectroscopy is in progress (Prescott et al., in preparation).

4.1.2. *PRG2*

PRG2 is a large Lyα nebula at $z \approx 2.27$ with a roughly diamond-shaped morphology in the B_W image (Figure 3). The identification of the strong line in the spectrum as Lyα is secure based on the fact that no other lines are well-detected in the discovery spectrum and corroborated by weak detections at the positions of C IV$\lambda\lambda$1548,1550, He IIλ1640, and C III]λ1909. In the case of [O II] at lower redshift, we would have easily detected [O III] and Hα instead. The Lyα nebula spans almost 100 kpc, and at the southwestern corner there is a very blue compact source that appears to be a Lyα-emitting galaxy from the spectrum. The redshift of this source is ideal for follow-up NIR spectroscopy as the rest-frame optical emission lines ([O II], [O III], Hβ, and Hα) will be observable in the J, H, and K bands. Continuum emission is observed from two compact knots located at either end and from spatially-extended emission at fainter levels in between them.

4.1.3. *PRG3*

PRG3 is a Lyα nebula at $z \approx 2.14$ (Figure 4). It has a rather clumpy horseshoe-shaped morphology in the B_W imaging and spans ≈74 kpc. The single strong line is identified as Lyα rather than [O II] based on the fact that we do not see corresponding detections of [O III] and Hα. The spectrum shows spatially-extended continuum, but no other strong emission lines.

4.1.4. *PRG4*

PRG4 appears to be a candidate that was selected due to a close grouping of compact blue sources (Figure 5). Due to the very blue color, it was flagged as a high priority target. At these wavelengths (blueward of the restframe wavelength of [O II]), Lyα is the only possible strong line. In addition, no other strong lines are seen in the spectrum. Although the B_W size of the full grouping is roughly $7''$, the observed Lyα at $z \approx 1.89$ is only marginally extended along the direction of the spectroscopic slit ($3.9''$, 33 kpc). The source may be larger in Lyα: there is additional diffuse emission outside the slit that is visible to the southwest in the B_W imaging, but without further spectroscopy, we cannot determine if it is associated with coincident Lyα emission.

4.1.5. *LABd05*

LABd05 is the source that was the inspiration for our broad-band Lyα nebula search (Figure 6; Dey et al. 2005). One of the largest Lyα nebulae known ($\gtrsim$ 100 kpc; Dey et al. 2005), it is located at $z \approx 2.656$. Our shallow MMT spectrum was taken at a slightly different position than the existing deeper spectroscopy from Keck but shows a hint of HeII emission and an emission line at 5081Å, both seen previously in the system (Dey et al. 2005). The emission line at 5081Å is thought to be Lyα from a background interloper galaxy at $z \approx 3.2$, the compact source that is visible in the ground-based imaging and located at the western edge of the slit for this observation. Detailed study of ground-based data as well as high resolution imaging from HST showed that there are numerous compact galaxies, including a spectroscopically-confirmed Lyman break galaxy, within the system that are offset spatially from the Lyα nebula itself (Dey et al. 2005; Prescott et al. 2012b). The HST imaging demonstrated that the nebula contains diffuse restframe UV continuum emission, that the Lyα emission itself is smooth with a relatively round and disk-like morphology, and that the HeII emission is spatially extended by $\approx 0.6-1''$ ($\approx 5-8$ kpc; Prescott et al. 2012b).

4.2. *Survey Contaminants*

The dominant contaminants in both the first and second priority spectroscopic samples are sources with spatially resolved blue continuum emission but no visible emission lines. Despite the lack of strong line emission in the B_W band, our morphological broad-band search selected these sources either due to sufficiently extended, blue continuum emission or due to a close projected grouping of blue galaxies. A few examples of these continuum-only sources are shown in Figure 7.

Without deeper spectroscopy, we can only speculate as to the nature of these continuum-only sources. The largest cases within the candidate sample (sources 1+2 and 3; Paper I) are so spatially extended (≈15-86″, which at $z \approx 1.2 - 2.9$ would imply physical sizes of $\approx 130 - 710$ kpc in the continuum) and irregular in morphology that they are almost certainly located within the Galaxy, perhaps low surface brightness Galactic reflection nebulae. Since low redshift ($z \lesssim 1.2$) blue star-forming populations or low surface brightness galaxies (LSBs) would be expected to show [OII], [OIII], or Hα emission lines in our spectra, some fraction of the remaining continuum-only contaminants may in fact be galaxies or Lyα nebulae in the redshift desert ($1.2 \lesssim z \lesssim 1.6$), for which Ly$\alpha$ is blueward of the atmospheric cut-off ($\lambda_{obs} \lesssim 3100$Å) but for which [OII] has been redshifted past the red end of our MMT/Blue Channel spectra ($\lambda_{obs} \gtrsim 8320$Å). One of the Ly$\alpha$ nebulae confirmed by our survey (PRG1, at $z \approx 1.67$) is in fact below the redshift where Lyα is covered by the B_W-band. Instead, this source was selected by our survey primarily due to blue continuum emission, and it was only thanks to the excellent blue sensitivity of MMT/Blue Channel that we were still able to detect the Lyα emission at ≈3250Å. The case of PRG1 lends credence to the hypothesis that at least a fraction of the continuum-only "contaminant" sources are in fact Lyα nebulae at $1.2 \lesssim z \lesssim 1.6$.

At the same time, however, our expectation from Paper I was that Lyα nebulae in the redshift desert should make up roughly 25% of the candidate sample, under the optimistic assumption that the Lyα nebula number density does not evolve significantly with redshift. In practice, we found continuum-only detections represented a much larger fraction (75%) of the target spectroscopic sample, suggesting that this explanation may not be the full story. While the presence of continuum emission in the spectra does confirm that these continuum-only sources are indeed real astrophysical objects and not artifacts within the NDWFS imaging, deeper ground-based optical spectroscopy or UV spectroscopy from space will be required to confirm their origin on a case by case basis. At this stage, their nature remains mysterious.

5. DISCUSSION

5.1. *A Successful Broad-band Lyα Nebula Survey*

This work is the first demonstration of the feasibility of conducting systematic surveys for large Lyα nebulae using deep broad-band imaging datasets. The primary advantage of our unusual survey approach is the enormous comoving volume that can be surveyed using deep archival datasets. In addition, since this search technique is best used in the blue where the sky is dark, the resulting Lyα nebula sample is weighted to lower redshifts ($z < 3$) where we have the opportunity to undertake detailed studies of their properties. The obvious trade-off is that our approach is not as sensitive to Lyα nebulae that are intrinsically faint, low surface-brightness, or compact in morphology, as discussed in Papers I and III. Our search, therefore, provides a measurement of the bright end of the Lyα nebula luminosity function, nicely complementing standard narrow-band surveys that probe to fainter luminosities.

The success rate for finding sources with Lyα emission was ≈ 27% for first priority and ≈ 20% for second priority candidates. Therefore, if we were able to target all the Lyα nebula candidates in our sample, we would expect to find a total of ≈ 18 Lyα nebulae (≈ 10 and ≈ 8 from the first and second priority set, respectively). While one of the goals of our broad-band survey for Lyα nebulae is to place constraints on the space density of these rare objects, a robust estimate of the space density requires a detailed analysis of the selection function and is beyond the scope of the present paper. Here, we briefly discuss our detection rate in the context of traditional narrowband Lyα nebula surveys.

Based on the results of the narrowband survey carried out at $z \approx 2.3$ by Yang et al. (2009), in Paper I we estimated the expected number of Lyα nebulae in our survey volume to be ∼60-400, assuming a 100% detection rate, the same detection limit as Yang et al. (2009), and a constant volume density as a function of redshift. Instead, we have confirmed 5 Lyα nebulae, and scaling these results to the unobserved candidates, we expect to find only 18. While this estimate is extremely crude, it does suggest that the space density of the detected Lyα nebulae in our sample is lower than that of the Yang et al. (2009) sample. Possible reasons for this difference are that (a) the Yang et al. (2009) narrow-band survey is more sensitive to fainter, and therefore less luminous, Lyα nebulae than our broad-band survey; (b) the Yang et al. (2009) survey does not exclude Lyα neb-

ulae with bright central sources whereas our survey does due to the nature of the morphological search algorithm; and/or (c) the Yang et al. (2009) survey is more sensitive to cosmic variance than our larger volume survey. We defer a more detailed discussion of the space density of Lyα nebulae implied by our survey to Paper III.

5.2. *Dispersion within the Lyα Nebula Class*

The power of a systematic survey is the opportunity it provides to find out what is common among a class of objects and also what the dispersion in properties is among members of that class. The four large cases in our sample (PRG1, PRG2, PRG3, LABd05) span nearly an order of magnitude in total Lyα luminosity ($50-170\times10^{42}$ erg s^{-1}), show a range of Lyα equivalent widths ($\sim 50-260$Å), and are at least $70-100$ kpc in diameter. Morphologically, the four large Lyα nebulae all show clumps and knots of emission in the broad-band imaging. The brightest compact knot in PRG1 is very red while that in PRG2 is remarkably blue. In addition, all four show what appears to be diffuse continuum emission in the ground-based spectroscopy. This could either be due to many unresolved clumps, or due to a continuum component that is truly spatially extended. Analysis of HST imaging of one system (LABd05) lends support to the latter hypothesis, revealing that most of the continuum in this one source is unresolved even at high resolution ($0.1''$; Prescott et al. 2012b). In three cases (PRG1, PRG2, LABd05) there is evidence for emission in other lines (e.g., CIV, HeII, or CIII]).

Given that diffuse continuum emission will have a larger impact on the observed broad-band color than line emission, one might ask if our survey is biased towards finding lower equivalent width sources than narrow-band surveys. In fact, however, Figure 8 shows that our survey uncovered Lyα nebulae with rest-frame equivalent widths comparable to those of luminous Lyα nebulae found using standard narrow-band surveys but over a much larger redshift range.

6. CONCLUSIONS

We have carried out an innovative and economical systematic search for large Lyα nebulae using archival deep, broad-band data. While our technique is only sensitive to the largest and brightest Lyα nebulae, it is able to probe enormous comoving volumes ($\approx 10^8$ h$_{70}^{-3}$ Mpc^3) using existing deep broad-band datasets. The details of our search algorithm, the selection function, and implied space density are discussed in Papers I and III of this series. In this paper (Paper II), we presented details of our spectroscopic follow-up of Lyα nebula candidates. Within our $\sim$8.5 square degree survey area and a redshift range of $z\approx1.6-2.9$, we confirmed 4 new Lyα nebulae and recovered 1 previously known case. The brightest 4 Lyα nebulae have Lyα luminosities of $\sim5-17\times10^{43}$ erg s^{-1} and sizes of $>$70 kpc. Our broad-band search found Lyα nebulae with large Lyα luminosities and equivalent widths comparable to those found with narrow-band surveys, but revealed a new common theme: at least some large Lyα nebulae show diffuse, spatially-extended continuum emission. The primary contaminants in our survey are sources that show nothing but blue continuum in the optical range, some of which we suspect may be galaxies or Lyα nebulae located in the redshift desert. Deep continuum spectroscopy and comparisons to *GALEX* photometry will be required to confirm this claim. This work uncovered the first example of a giant Lyα nebula at $z<2$ and has demonstrated the feasibility of using deep broad-band datasets to efficiently locate luminous Lyα nebulae within enormous comoving volumes.

We are grateful to Christy Tremonti and Kristian Finlator for observing assistance and to the telescope operators at the MMT, in particular Ale Milone and John McAfee. We would also like to thank the Steward Observatory TAC for the generous allocations of MMT time used in support of this project, as well as the anonymous referee for helpful suggestions. This research draws upon data from the NOAO Deep Wide-Field Survey (NDWFS) as distributed by the NOAO Science Archive. NOAO is operated by the Association of Universities for Research in Astronomy (AURA), Inc. under a cooperative agreement with the National Science Foundation. M. P. was supported by a NSF Graduate Research Fellowship and a TABASGO Prize Postdoctoral Fellowship. A. D. and B. T. J.'s research is supported by NOAO, which is operated by AURA under a cooperative agreement with the National Science Foundation.

REFERENCES

Barrio, F. E., et al. 2008, Monthly Notices of the Royal Astronomical Society, 389, 792
Basu-Zych, A., & Scharf, C. 2004, The Astrophysical Journal, 615, L85
Bertin, E., & Arnouts, S. 1996, Astronomy and Astrophysics Supplement, 117, 393
Chapman, S. C., Scott, D., Windhorst, R. A., Frayer, D. T., Borys, C., Lewis, G. F., & Ivison, R. J. 2004, The Astrophysical Journal, 606, 85
Colbert, J. W., Scarlata, C., Teplitz, H., Francis, P., Palunas, P., Williger, G. M., & Woodgate, B. 2011, The Astrophysical Journal, 728, 59
Dey, A., et al. 2005, The Astrophysical Journal, 629, 654
Faucher-Giguère, C.-A., Kereš, D., Dijkstra, M., Hernquist, L., & Zaldarriaga, M. 2010, The Astrophysical Journal, 725, 633
Francis, P. J., et al. 1996, The Astrophysical Journal, 457, 490
Geach, J. E., Smail, I., Chapman, S. C., Alexander, D. M., Blain, A. W., Stott, J. P., & Ivison, R. J. 2007, The Astrophysical Journal, 655, L9
Geach, J. E., et al. 2009, The Astrophysical Journal, 700, 1
Goerdt, T., Dekel, A., Sternberg, A., Ceverino, D., Teyssier, R., & Primack, J. R. 2010, Monthly Notices of the Royal Astronomical Society, 407, 613
Haberzettl, L., Bomans, D. J., Dettmar, R.-J., & Pohlen, M. 2007, Astronomy and Astrophysics, 465, 95
Ivison, R. J., Smail, I., Le Borgne, J.-F., Blain, A. W., Kneib, J.-P., Bezecourt, J., Kerr, T. H., & Davies, J. K. 1998, Monthly Notices of the Royal Astronomical Society, 298, 583
Jannuzi, B. T., & Dey, A. 1999, in Photometric Redshifts and the Detection of High Redshift Galaxies, ed. R. Weymann, R., Storrie-Lombardi, L., Sawicki, M., & Brunner, Vol. 191 (Astronomical Society of the Pacific Conference Series), 111
Matsuda, Y., Iono, D., Ohta, K., Yamada, T., Kawabe, R., Hayashino, T., Peck, A. B., & Petitpas, G. R. 2007, The Astrophysical Journal, 667, 667
Matsuda, Y., et al. 2004, The Astronomical Journal, 128, 569
Matsuda, Y., et al. 2005, The Astrophysical Journal, 634, L125
Matsuda, Y., et al. 2011, Monthly Notices of the Royal Astronomical Society: Letters, 410, L13
McCarthy, P. J. 1993, Annual Review of Astronomy and Astrophysics, 31, 639
Miley, G. K., et al. 2006, The Astrophysical Journal, 650, L29

Table 1
Observing Log

UT Date	Instrumental Resolution[a] (arcsec)	Unvignetted Slit (Å)	Spatial Binning (arcsec/pixel)	Seeing (arcsec)	Conditions
2007 May 20	2.6	1.0×120	0.56	1.0-1.2	Clear, high winds
2007 May 21	2.6	1.0×120	0.56	1.0-1.2	Clear, high winds
2007 May 22	3.4	1.5×120	0.56	1.3-1.7	Clear, high winds
2008 April 3	3.4	1.5×120	0.28	1.0	Mostly clear
2008 April 30	3.4	1.5×120	0.28	1.2-1.9	Clear, high winds
2008 June 8	3.4	1.5×120	0.28	1.0	Clear
2008 June 9	3.4	1.5×120	0.28	1.1-2.0	Clear, high winds

[a] Quoted instrumental resolution is the average of measurements of the Hg Iλ4047, Hg Iλ4358, Hg Iλ5461, and O Iλ5577 sky lines.

Nilsson, K. K., Fynbo, J. P. U., Mø ller, P., Sommer-Larsen, J., & Ledoux, C. 2006, Astronomy and Astrophysics, 452, L23

Oke, J. B. 1974, The Astrophysical Journal Supplement Series, 27, 21

Palunas, P., Teplitz, H. I., Francis, P. J., Williger, G. M., & Woodgate, B. E. 2004, The Astrophysical Journal, 602, 545

Prescott, M. K. M. 2009, Phd, University of Arizona

Prescott, M. K. M., Dey, A., & Jannuzi, B. T. 2009, The Astrophysical Journal, 702, 554

Prescott, M. K. M., Dey, A., & Jannuzi, B. T. 2012a, The Astrophysical Journal, 748, 125

Prescott, M. K. M., Kashikawa, N., Dey, A., & Matsuda, Y. 2008, The Astrophysical Journal, 678, L77

Prescott, M. K. M., et al. 2012b, The Astrophysical Journal, 752, 86

Rosdahl, J., & Blaizot, J. 2012, Monthly Notices of the Royal Astronomical Society, 423, 344

Saito, T., Shimasaku, K., Okamura, S., Ouchi, M., Akiyama, M., & Yoshida, M. 2006, The Astrophysical Journal, 648, 54

Saito, T., Shimasaku, K., Okamura, S., Ouchi, M., Akiyama, M., Yoshida, M., & Ueda, Y. 2008, The Astrophysical Journal, 675, 1076

Smith, D. J. B., & Jarvis, M. J. 2007, Monthly Notices of the Royal Astronomical Society: Letters, 378, L49

Smith, D. J. B., Jarvis, M. J., Lacy, M., & Martínez-Sansigre, A. 2008, Monthly Notices of the Royal Astronomical Society, 389, 799

Smith, D. J. B., Jarvis, M. J., Simpson, C., & Martínez-Sansigre, A. 2009, Monthly Notices of the Royal Astronomical Society, 393, 309

Steidel, C. C., Adelberger, K. L., Shapley, A. E., Pettini, M., Dickinson, M., & Giavalisco, M. 2000, The Astrophysical Journal, 532, 170

Taniguchi, Y., & Shioya, Y. 2000, The Astrophysical Journal, 532, L13

Taniguchi, Y., Shioya, Y., & Kakazu, Y. 2001, The Astrophysical Journal, 562, L15

Valdes, F. 1992, Astronomical Data Analysis Software and Systems I, 25

van Ojik, R., Roettgering, H. J. A., Carilli, C. L., Miley, G. K., Bremer, M. N., & Macchetto, F. 1996, Astronomy and Astrophysics

Webb, T. M. A., Yamada, T., Huang, J.-S., Ashby, M. L. N., Matsuda, Y., Egami, E., Gonzalez, M., & Hayashimo, T. 2009, The Astrophysical Journal, 692, 1561

Weidinger, M., Mø ller, P., Fynbo, J. P. U., & Thomsen, B. 2005, Astronomy and Astrophysics, 436, 825

Yang, Y., Zabludoff, A., Eisenstein, D., & Davé, R. 2010, The Astrophysical Journal, 719, 1654

Yang, Y., Zabludoff, A., Tremonti, C., Eisenstein, D., & Davé, R. 2009, The Astrophysical Journal, 693, 1579

Zirm, A. W., Dey, A., Dickinson, M., & Norman, C. J. 2009, The Astrophysical Journal, 694, L31

Table 2
Spectroscopic Targets

	Candidate Name	Right Ascension (hours)	Declination (degrees)	Priority	UT Date	Exposure Time (s)	Class[a]	Notes
(2)	NDWFS J143006.9+353437	14:30:06.864	35:34:36.73	3	2007 May 20-21	2400	Continuum	Galactic?
(3)	NDWFS J142846.2+330819	14:28:46.228	33:08:19.42	3	2007 May 20-21	10800	Continuum	Galactic?
(10)	NDWFS J143411.0+331731	14:34:10.975	33:17:31.26	1	2007 May 20	1800	Lyα	LABd05
(14)	NDWFS J143512.3+351109	14:35:12.336	35:11:08.62	2	2008 Jun 8-9	7200	Lyα	PRG1
(18)	NDWFS J143222.8+324943	14:32:22.768	32:49:42.67	2	2008 Jun 8	1800	Continuum	-
(24)	NDWFS J142614.7+344434	14:26:14.714	34:44:34.22	1	2008 Jun 8	3600	Continuum	-
(26)	NDWFS J142622.9+351422	14:26:22.905	35:14:22.02	1	2008 Apr 3	3600	Lyα	PRG2
(29)	NDWFS J142526.3+335112	14:25:26.332	33:51:12.16	1	2008 Jun 9	3600	Continuum	-
(31)	NDWFS J142547.1+334454	14:25:47.126	33:44:54.13	1	2008 Apr 30	2400	Continuum	-
(33)	NDWFS J142714.8+343155	14:27:14.791	34:31:54.55	2	2008 Jun 8	1800	Continuum	-
(34)	NDWFS J143128.2+352658	14:31:28.245	35:26:57.91	2	2007 May 22	5400	Continuum	-
(40)	NDWFS J142653.2+343855	14:26:53.172	34:38:55.39	1	2008 Apr 30	3600	Lyα	PRG4
(44)	NDWFS J142927.8+345906	14:29:27.837	34:59:06.14	3	2007 May 21	3600	Continuum	-
(52)	NDWFS J143706.6+335653	14:37:06.588	33:56:52.65	2	2007 May 20-21	4800	Continuum	-
(58)	NDWFS J142516.6+324335	14:25:16.629	32:43:35.47	1	2008 Jun 8	3600	Continuum	-
(59)	NDWFS J143412.7+332939	14:34:12.722	33:29:39.19	1	2008 May 20	10800	Lyα	PRG3
(65)	NDWFS J143207.2+343101	14:32:07.224	34:31:01.34	3	2007 May 22	3600	Continuum	-
(66)	NDWFS J142539.9+344959	14:25:39.859	34:49:59.19	1	2008 Jun 8	3600	Continuum	-
(70)	NDWFS J142753.8+341204	14:27:53.762	34:12:04.10	1	2007 May 20-21	8400	Continuum	-
(71)	NDWFS J142600.8+350252	14:26:00.842	35:02:52.36	3	2008 Apr 3	3600	Continuum	-
(72)	NDWFS J142643.9+340937	14:26:43.850	34:09:36.82	1	2008 Jun 9	3600	Continuum	-
(73)	NDWFS J142722.4+345225	14:27:22.408	34:52:24.74	1	2008 Apr 3	3600	Continuum	-
(74)	NDWFS J142620.0+340427	14:26:19.982	34:04:27.01	1	2008 Apr 30	2400	Continuum	-
(80)	NDWFS J142548.3+322957	14:25:48.283	32:29:56.58	1	2008 Jun 9	3600	Continuum	-
(82)	NDWFS J142449.8+324743	14:24:49.761	32:47:42.61	1	2008 Apr 30	3600	Continuum	-
(85)	NDWFS J142533.0+343912	14:25:32.966	34:39:11.95	3	2008 Apr 3	3600	Continuum	-

Candidate ID numbers in the first column are the same as in Paper I.
[a] Spectroscopic targets were classified as either showing "Lyα" or "Continuum" emission.

Table 3
Lyα Nebula Measurements

	PRG1	PRG2	PRG3	PRG4	LABd05
Aperture (arcsec)	1.5 × 5.04	1.5 × 7.84	1.0 × 5.60	1.5 × 1.68	1.0 × 4.48
$\lambda_{Ly\alpha,obs}$ (Å)	3249.61 ± 0.39	3971.41 ± 0.13	3813.28 ± 0.90	3511.23 ± 0.67	4444.99 ± 0.31
Redshift	1.6731 ±0.0003	2.2668 ±0.0001	2.1368 ±0.0007	1.8883 ±0.0005	2.6564 ±0.0003
$F_{Ly\alpha}$ (10^{-17} erg s^{-1} cm^{-2})	44.1 ± 4.0	49.2 ± 1.1	10.2 ± 1.2	10.3 ± 1.2	19.0 ± 0.9
$L_{Ly\alpha}$ (10^{42} erg s^{-1})	8.2 ± 0.7	19.3 ± 0.4	3.5 ± 0.4	2.6 ± 0.3	10.9 ± 0.5
Lyα EW$_{rest}$ (Å)	257.1 ± 29.1	127.3 ± 6.3	47.1 ± 6.4	88.7 ± 11.8	115.5 ± 9.5
Lyα FWHM$_{obs}$ (Å)	9.19 ± 0.60	8.52 ± 0.19	23.36 ± 7.90	6.51 ± 0.89	15.44 ± 0.70
Lyα σ_v (km s^{-1})	361.2 ± 23.7	273.9 ± 6.1	782.1 ± 264.3	236.8 ± 32.2	443.3 ± 20.0
$F_{CIV\lambda1550}$ (10^{-17} erg s^{-1} cm^{-2})[a]	2.1 ± 1.1	1.8 ± 0.8	< 0.8	< 0.8	< 5.4
$F_{HeII\lambda1640}$ (10^{-17} erg s^{-1} cm^{-2})[a]	5.8 ± 1.0	1.8 ± 0.9	< 0.9	0.7 ± 0.5	1.4 ± 1.3
$F_{CIII\lambda1909}$ (10^{-17} erg s^{-1} cm^{-2})[a]	4.8 ± 0.9	3.0 ± 1.1	< 1.5	< 1.4	< 1.8
B_W Diameter Along Slit[b] (arcsec)	8.96	10.12	6.72	6.75	9.32
B_W Isophotal Area[b] (arcsec^2)	40.9	73.2	45.3	38.7	54.4
B_W Surface Brightness[b] (mag arcsec^{-2})	27.2	27.0	26.8	27.0	27.0
Lyα Diameter Along Slit[c] (arcsec)	9.24	12.04	8.96	3.92	8.96
Lyα Diameter Along Slit[c] (kpc)	78.3	99.0	74.4	33.0	71.3
Approximate Lyα Isophotal Area[d] (arcsec^2)	43.4	103.7	80.4	>5.9[f]	50.3
Approximate Total $L_{Ly\alpha}$[e] (10^{42} erg s^{-1})	47.2 ± 4.3	170.2 ± 3.7	49.6 ± 6.1	>2.6[f]	122.8 ± 6.0

[a] Line flux upper limits are 2σ values.
[b] B_W sizes, isophotal areas, and surface brightnesses measured from the NDWFS imaging using SourceExtractor with a detection threshold of 28.9 mag arcsec^{-2}, the median 1σ B_W surface brightness limit of NDWFS.
[c] Lyα sizes measured from the 2D spectra using SourceExtractor with detection thresholds of [2.5, 1.0, 0.8, 2.1, 1.5]$\times10^{-18}$ erg s^{-1} cm^{-2} Å^{-1} arcsec^{-2}, the respective 1σ line surface brightness limits at the position of Lyα.
[d] Approximate Lyα isophotoal area computed by correcting the B_W isophotal area A_{B_W} by a factor of ν^2, where ν is the ratio of the Lyα and B_W diameters measured along the slit.
[e] Approximate total Lyα luminosity computed by scaling the Lyα luminosity measured within the spectroscopic aperture by a geometric correction factor of $f_{geo} = A_{B_W} \times \nu^2/(\omega \times d)$, where A_{B_W} is the isophotal area of the source on the B_W image, ν is the ratio of the Lyα and B_W diameters measured along the slit, ω is the slit width, and d is the spatial extent of the spectral extraction aperture.
[f] As the B_W emission is not an accurate tracer of the Lyα emission in PRG4, approximate luminosity and area estimates have been replaced with lower limits derived from the spectroscopic data alone.

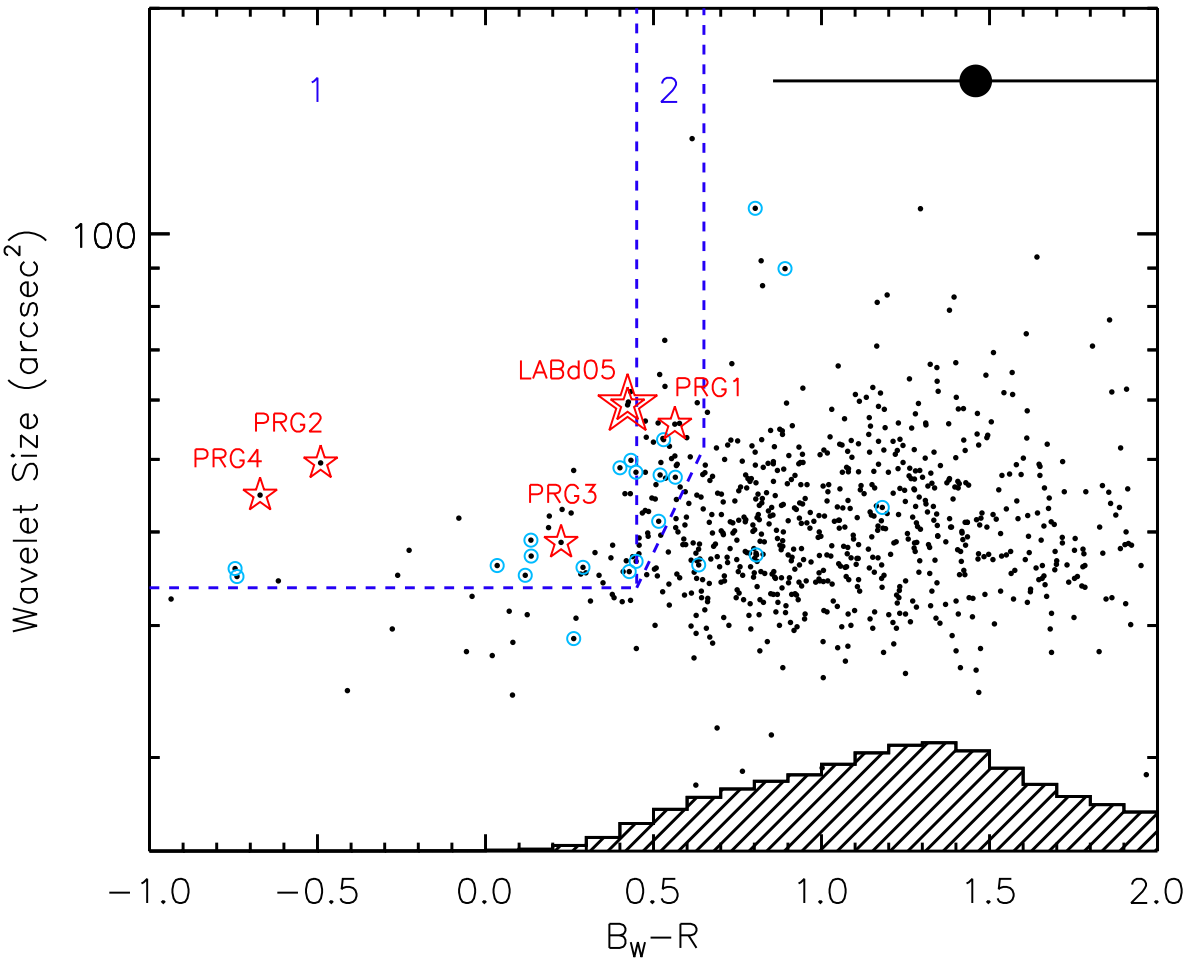

Figure 1. Size vs. $B_W - R$ color of Lyα nebula candidates selected using the broad-band morphological search pipeline. The wavelet size corresponds to the size of the source in the wavelet power map, but does not indicate the true nebular size of the object (Paper I). All candidates are shown as filled black circles. The first and second priority selection regions indicated (blue dashed lines) contain 39 and 40 Lyα nebula candidates, respectively. The spectroscopic targets that showed Lyα are indicated using red stars, and those that did not show Lyα are marked with light blue circles. The large filled black circle with an error bar represents the typical color of low surface brightness galaxies (LSBs; Haberzettl et al. 2007), and the histogram (plotted on a linear scale) represents the distribution of $B_W - R$ colors for field galaxies in NDWFS, demonstrating that the colors of our final Lyα nebula candidates are substantially bluer than typical LSBs and field galaxies.

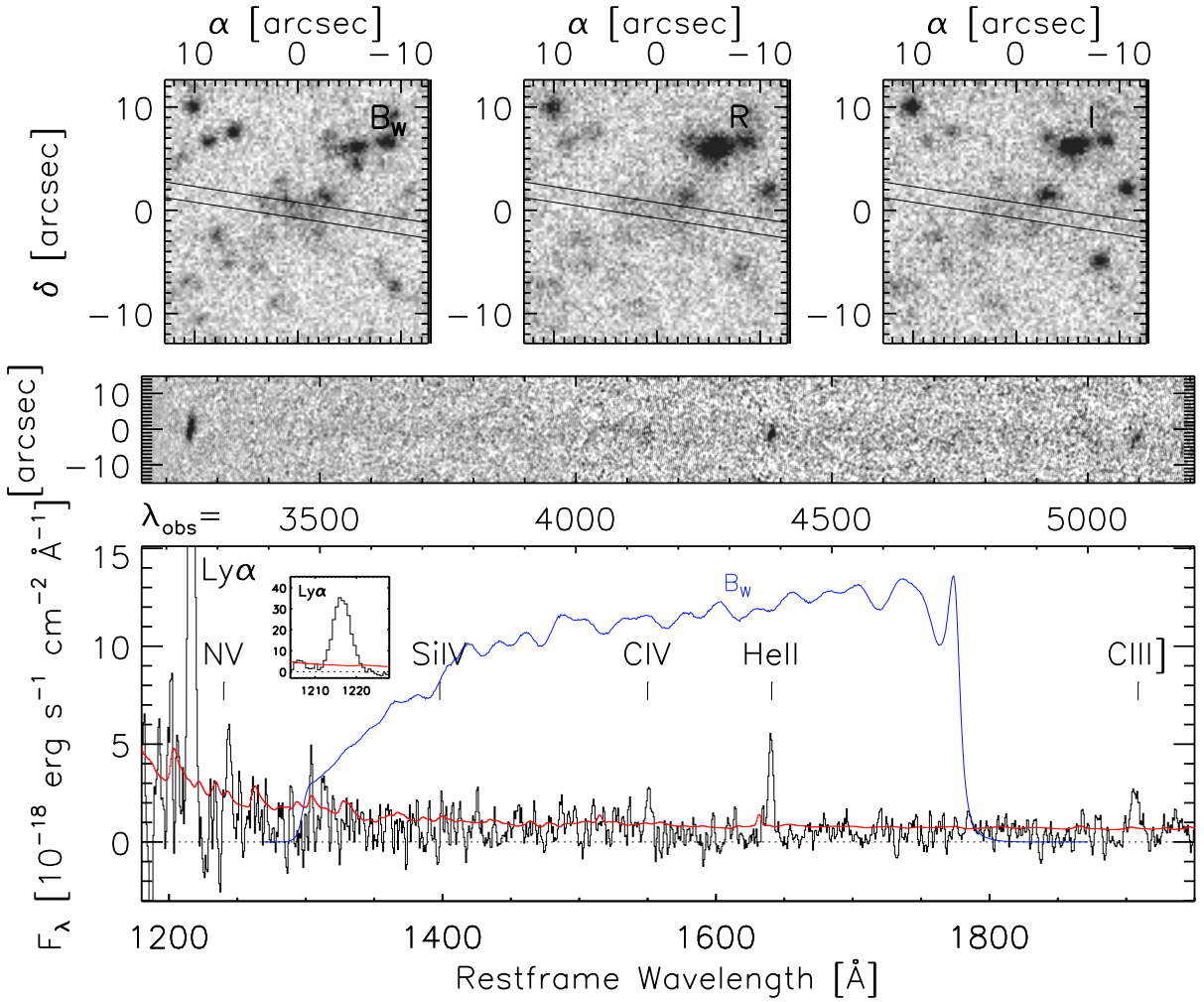

Figure 2. Imaging and MMT spectroscopic observations of PRG1, a Lyα nebula at $z \approx 1.67$. The top row shows the optical B_W, R, and I imaging along with the slit used for follow-up spectroscopy. The central panel contains the two-dimensional spectrum versus observed wavelength, and the bottom panel presents the one-dimensional spectrum extracted from a $1.5{\times}5.04''$ aperture. The error spectrum (red line) and B_W bandpass (blue line) are shown, and the positions of common emission lines are indicated. The one-dimensional Lyα emission line profile is shown in the inset panel. Spectroscopic data presented are from the second night of observations only (UT 2008 June 9; for details see Prescott et al. 2009).

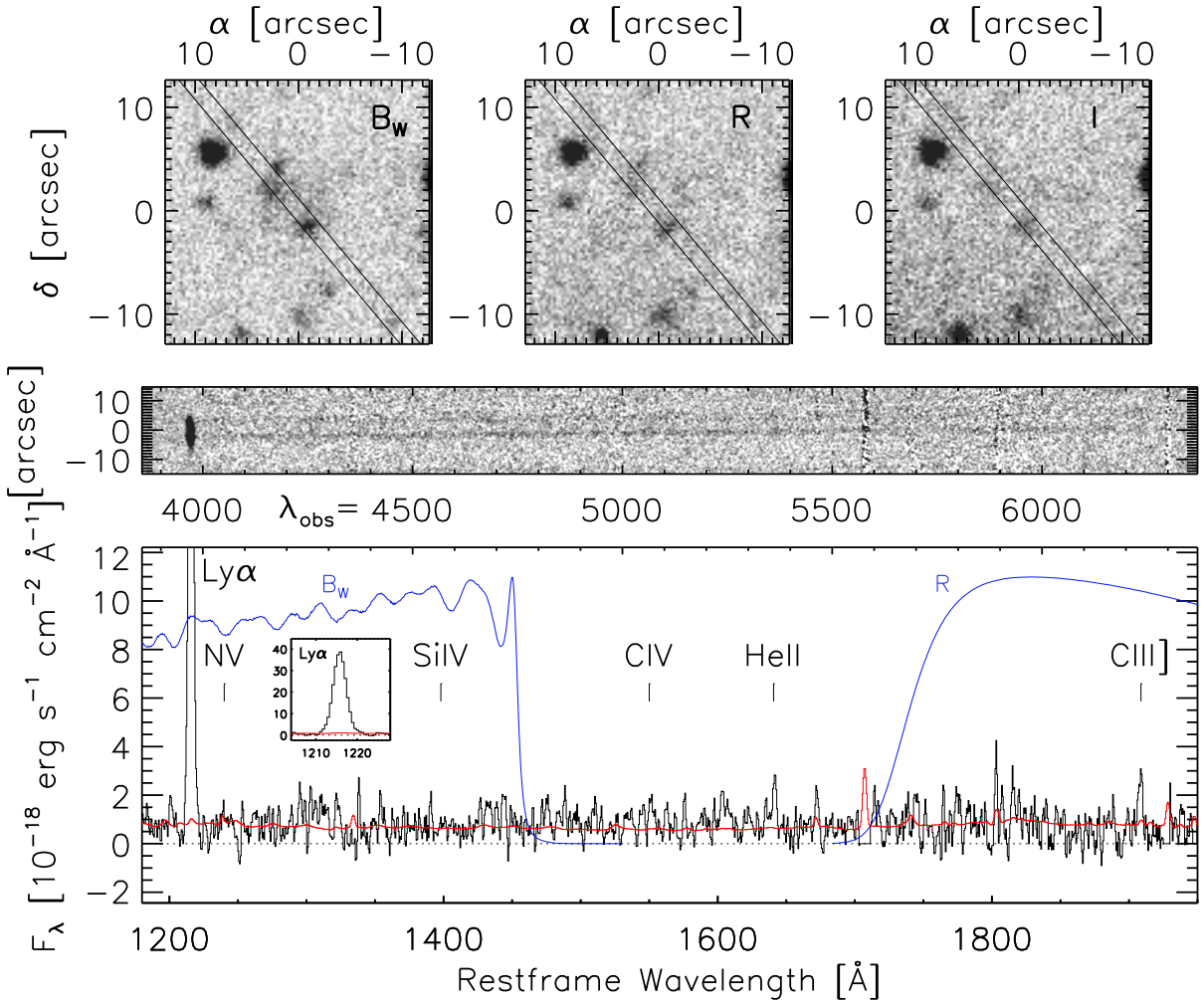

Figure 3. Imaging and MMT spectroscopic observations of PRG2, a Lyα nebula at $z \approx 2.27$. The top row shows the optical B_W, R, and I imaging along with the slit used for follow-up spectroscopy. The central panel contains the two-dimensional spectrum versus observed wavelength, and the bottom panel presents the one-dimensional spectrum extracted from a $1.5\times7.84''$ aperture. The error spectrum (red line) and B_W and R bandpasses (blue lines) are shown, and the positions of common emission lines are indicated. The one-dimensional Lyα emission line profile is shown in the small inset panel.

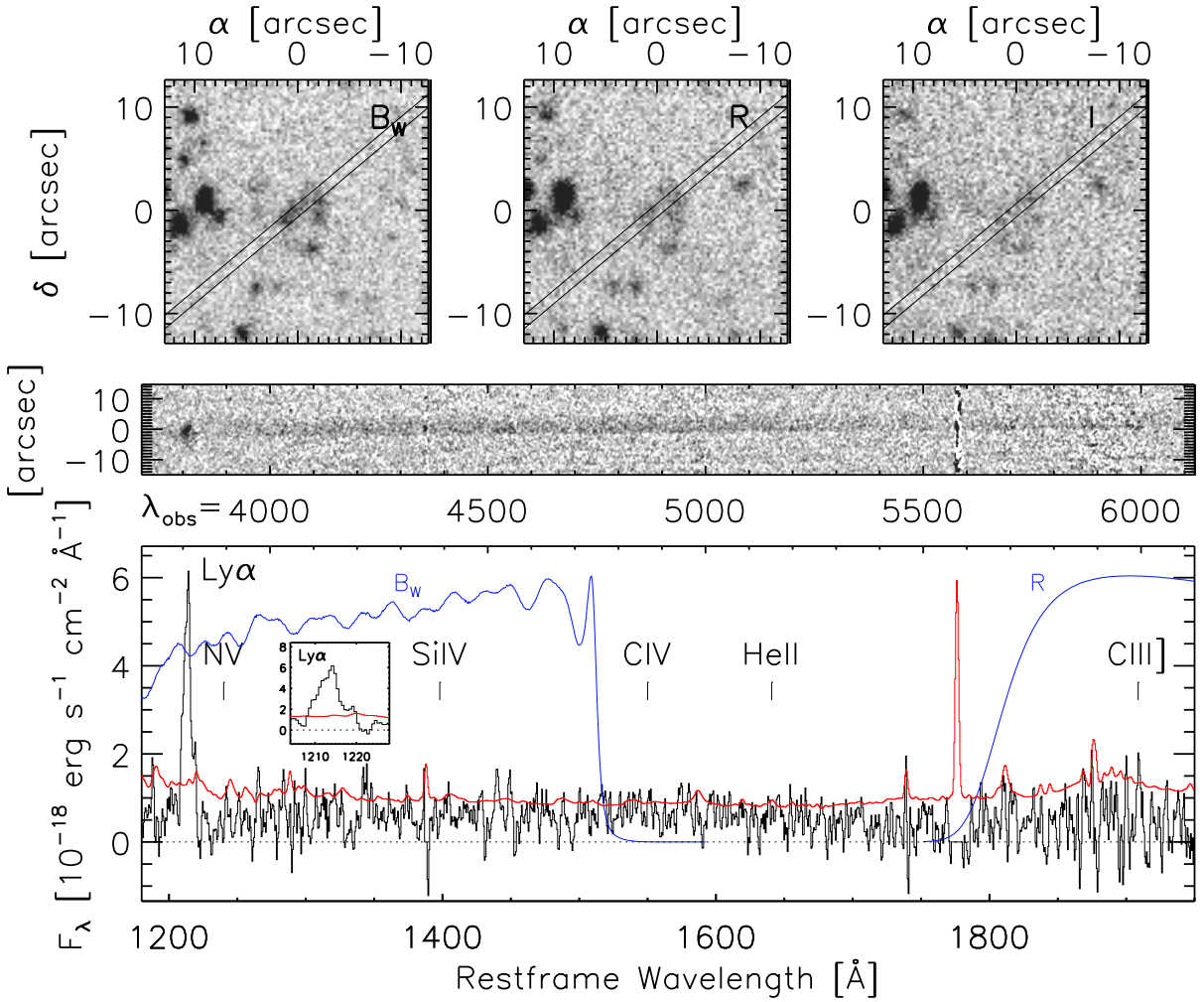

Figure 4. Imaging and MMT spectroscopic observations of PRG3, a Lyα nebula at $z \approx 2.14$. The top row shows the optical B_W, R, and I imaging along with the slit used for follow-up spectroscopy. The central panel contains the two-dimensional spectrum versus observed wavelength, and the bottom panel presents the one-dimensional spectrum extracted from a $1.0\times5.6''$ aperture. The error spectrum (red line) and B_W and R bandpasses (blue lines) are shown, and the positions of common emission lines are indicated. The one-dimensional Lyα emission line profile is shown in the small inset panel.

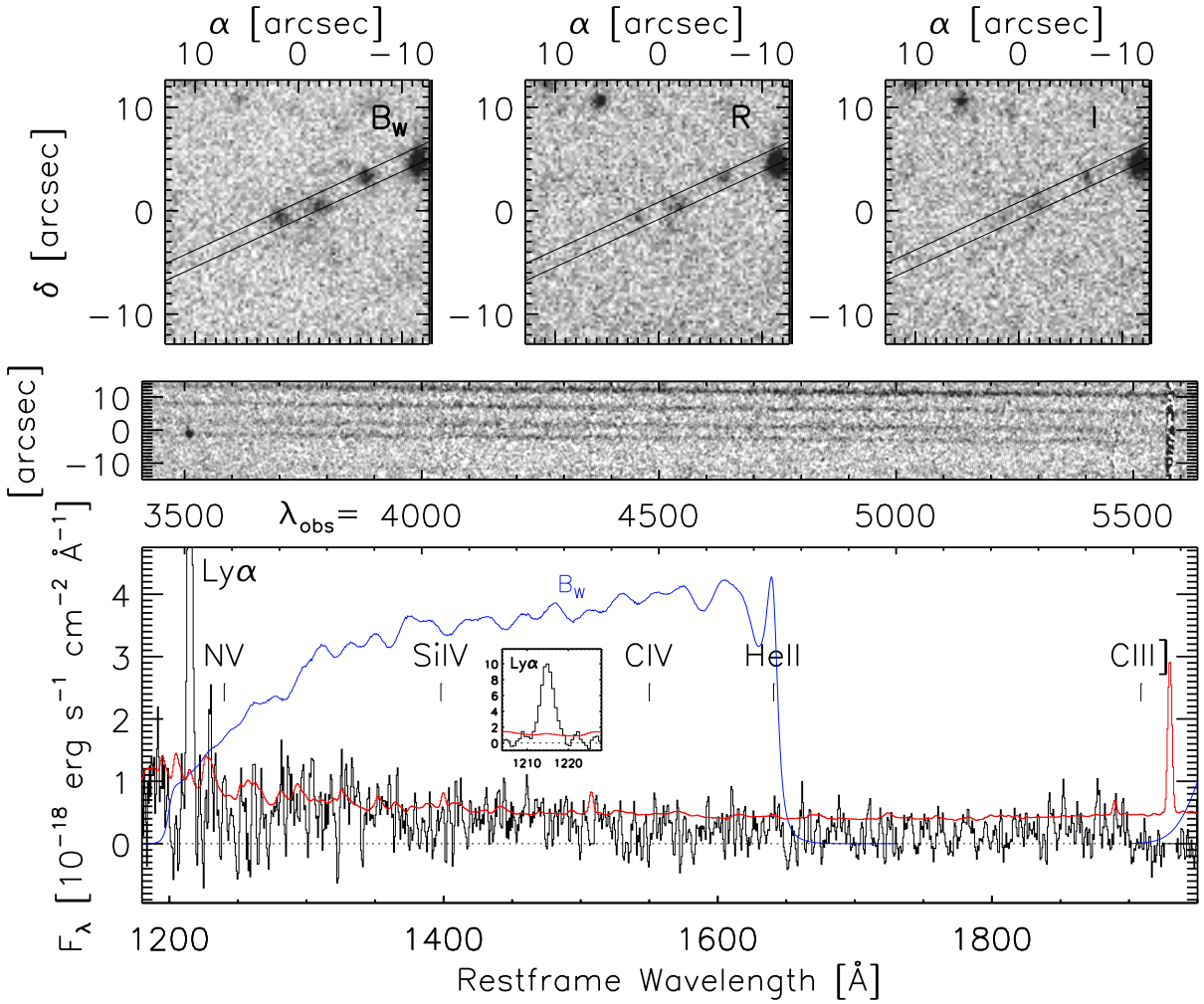

Figure 5. Imaging and MMT spectroscopic observations of PRG4, a Lyα nebula at $z \approx 1.89$. The top row shows the optical B_W, R, and I imaging along with the slit used for follow-up spectroscopy. The central panel contains the two-dimensional spectrum versus observed wavelength, and the bottom panel presents the one-dimensional spectrum extracted from a $1.5\times1.68''$ aperture. The error spectrum (red line) and B_W and R bandpasses (blue lines) are shown, and the positions of common emission lines are indicated. The one-dimensional Lyα emission line profile is shown in the small inset panel. The size of PRG4 is unknown; the source is very compact along the spectroscopic slit, but additional diffuse emission that may or may not be Lyα is visible to the south in the B_W imaging.

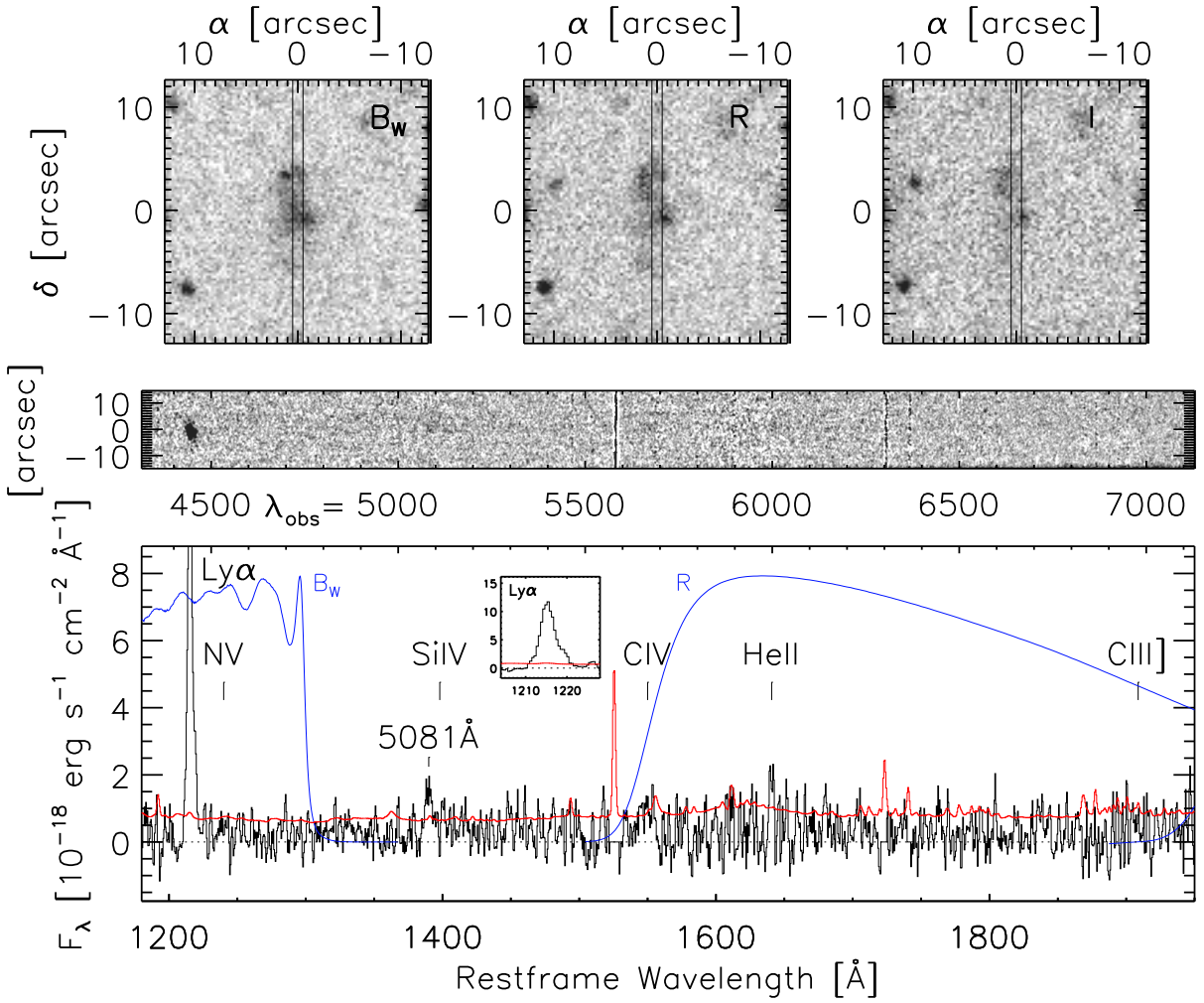

Figure 6. Imaging and MMT spectroscopic observations of LABd05, a previously-known Lyα nebula at $z \approx 2.656$ (Dey et al. 2005). The top row shows the optical B_W, R, and I imaging along with the slit used for follow-up spectroscopy. The central panel contains the two-dimensional spectrum versus observed wavelength and the bottom panel presents the one-dimensional spectrum extracted from a $1.0\times4.48''$ aperture. The error spectrum (red line) and B_W and R bandpasses (blue lines) are shown, and the positions of common emission lines are indicated. The one-dimensional Lyα emission line profile is shown in the small inset panel. The emission line at 5081Å from a background galaxy at $z \approx 3.2$ is labeled for reference (Dey et al. 2005).

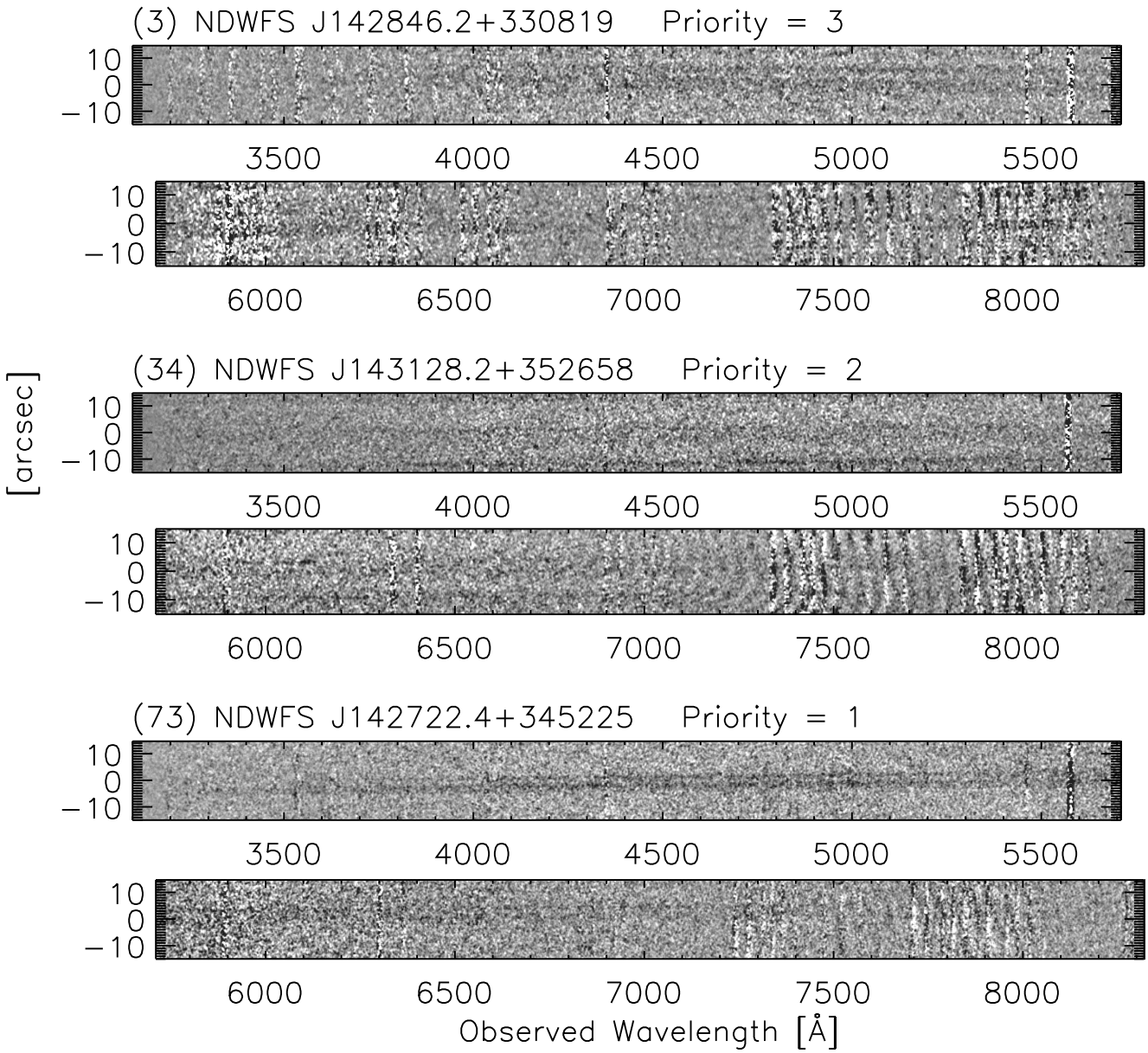

Figure 7. Examples of the continuum-only contaminant sources discussed in the text (Section 4.2). Two-dimensional MMT/Blue Channel Spectrograph spectra are shown versus observed wavelength, with the target source centered at $0''$ along the spatial dimension.

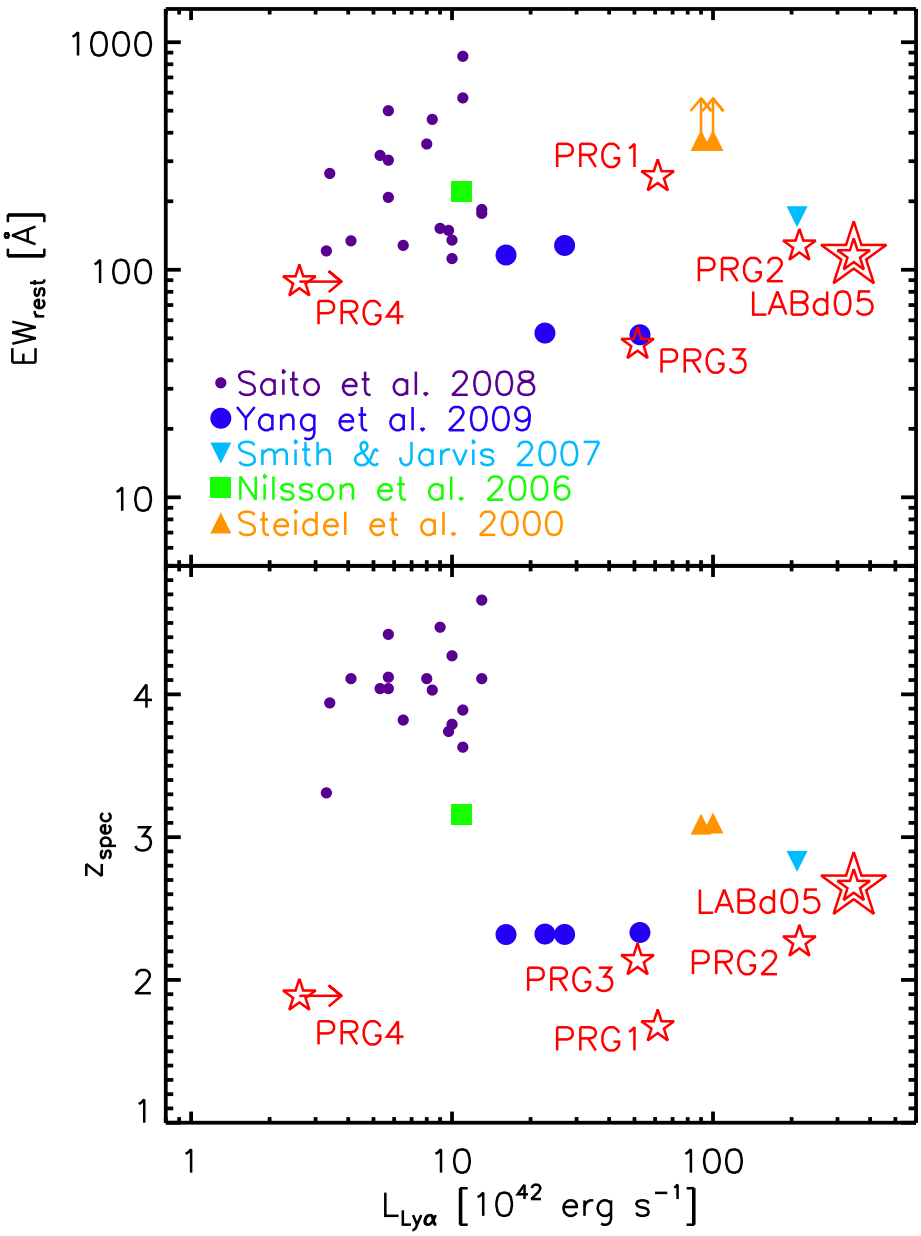

Figure 8. Rest-frame equivalent width (EW_{rest}, top panel) and spectroscopic redshift (z_{spec}, bottom panel) versus total Lyα luminosity ($L_{Ly\alpha}$) for Lyα nebulae reported in the literature (Steidel et al. 2000; Nilsson et al. 2006; Smith & Jarvis 2007; Saito et al. 2008; Yang et al. 2009) and those found using our broad-band search (red stars). Our survey succeeded in discovering Lyα nebulae with rest-frame equivalent widths comparable to those found by previous narrow-band surveys, but covers a large redshift range using just a single broad-band filter.